# AN EXPERIMENTAL STUDY OF THE EFFECTS OF DIAGENETIC CLAY MINERALS ON RESERVOIR SANDS

PAUL H. NADEAU†

Exxon Production Research Company, P.O. Box 2189, Houston, Texas 77252-2189

Abstract—Despite substantial scientific research efforts, accurate determination of the petrophysical effects of clay minerals on reservoir sands remains problematic. Diagenetic clays such as smectite and illite are of particular interest because of the pronounced effects these clays can have on reservoir quality. Here, results are reported from an experimental study based on the hydrothermal growth of smectite in synthetic sands. The sands contained quartz, dolomite and kaolinite, and were reacted at 175–200 °C, for 19–45 d. The hydrothermal reaction can be written as follows:

$$\text{dolomite} + \text{kaolinite} + \text{quartz} \rightarrow \text{smectite} + \text{calcite} + CO_2$$
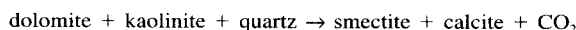
X-ray diffraction (XRD), electron microprobe (EMP) and electron diffraction (ED) analysis show that the synthetic Mg-rich smectite formed is saponite, with a cation exchange capacity (CEC) of about 100 meq/ 100 g. After reaction, brine permeability reductions of up to 98% were observed from the growth of less than 5% smectite. Scanning electron microscopy (SEM) observations of critical-point-dried reacted samples show that the clay behaves as a pervasive microporous cement with a complex pore-bridging texture affecting most of the available pore space. Morphologically, the clay is similar to naturally occurring diagenetic smectite from Gulf Coast sandstone reservoirs. The delicate clay texture collapses during air-drying and forms pore-lining masses. This phenomenon is similar to that observed for air-dried reservoir samples which contain dispersed diagenetic clays. An air-dried sample, then resaturated with brine, showed a marked increase in permeability. This increase is associated with the irreversible collapse of the clay texture. The experimental results indicate that the growth of diagenetic clay can severely reduce formation permeability, even at very low clay contents. The results also demonstrate the utility of hydrothermal experimental petrophysics for investigating the effects of diagenesis on rock properties.

Key Words—Diagenetic Clay, Experimental Petrophysics, Permeability, Reservoir Quality.

INTRODUCTION

A problematic aspect of evaluating hydrocarbon-bearing sandstone is to accurately model the effects of clay and shale components on reservoir properties. Clay minerals and other sedimentary materials can exist in sandstone reservoirs as detrital shale components in the form of shale laminae, structural clasts and dispersed shale matrix. Clay minerals are also commonly present as authigenic/diagenetic clays which have formed within the sandstone. These include pore-filling kaolinite, pore-lining chlorite and pore-bridging illite (Wilson and Pittman 1977). Core-based studies of the effects of clay and shale on reservoir sandstones are complicated by a number of factors. These include detection and accurate quantification of the clay content, types and distribution within the reservoir; sample heterogeneity; drilling mud contamination and invasion damage; and alteration of clay microstructure and wettability by conventional air-drying methods and hydrocarbon extraction procedures. These obstacles make it extremely difficult, if not impossible, to isolate the effects of interest as a function of clay content. This is particularly true for diagenetic clays such as illite and smectite that have formed within the sandstone after the time of deposition, and which are con-

sidered to have large effects on rock properties even at very low contents. ("Smectite" refers to a group of expandable clay minerals that includes montmorillonite, beidellite, nontronite and saponite.)

Previous studies of "delicate" diagenetic clays have often dealt with illite and mixed-layered illite–smectite (McHardy et al. 1982; Pallatt et al. 1984; deWaal et al. 1988). These studies have shown that:

1) Small amounts of diagenetic clay can greatly reduce sandstone permeabilities.
2) The delicate clay morphology can collapse on air-drying of core samples.
3) The effects are commonly underestimated by conventional core analysis techniques.

In order to circumvent the difficulties of core-based studies mentioned earlier, a research program based on experimental petrophysics was developed to directly determine the effects of clay diagenesis using hydrothermal mineral reactions in synthetic sandstones. The preliminary results of this study are presented here.

EXPERIMENTAL METHODS

Hydrothermal Reaction and Sample Preparation

The mineral reaction utilized was chosen because it requires a relatively low temperature and short run times, involves common sedimentary minerals and

---

† Present Address: Statoil, N-4035 Stavanger, Norway.

18

Table 1. Minerals used to make synthetic sandstones.

Mineral	Composition ideal	Particle size μm	Density g cm^{-3}
Quartz	SiO_2	less than 100	2.65
Kaolinite	$Al_4Si_4O_{10}(OH)_8$	less than 4	2.62
Dolomite	$CaMg(CO_3)_2$	106–45	2.87

Source: quartz = Fisher silica 140 mesh; kaolinite = Clay Minerals Society, Source Clay Standard KGa-1, well-crystallized Georgia kaolinite; dolomite = Wards, specimen from Selasvann, Norway.

produces high-surface-area smectite clay (W. L. Huang, 1988 personal communication).

The reaction can be written as follows:

$$\text{dolomite + kaolinite + quartz} \rightarrow \text{smectite} + \text{calcite} + CO_2 \qquad [1]$$
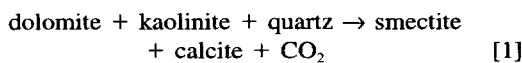
The reaction was typically performed in 250-mL stainless steel hydrothermal reaction vessels at temperatures of to 200 °C (392 °F) for periods between 19 and 45 d.

The minerals used to fabricate the synthetic sandstones are listed in Table 1 along with their ideal chemical formulae. The nominal reaction mix consisted of, by weight, 90% quartz, 5% dolomite and 5% kaolinite. The minerals were first combined and homogenized in a dry state. Approximately 4 mL of brine was then stirred into the mix. The resulting mixture was placed into a die and formed into a cylinder by applying 335 bar (5000 psi) using a hydraulic press. The cylindrical sample is approximately 2.5 cm in diameter and 3.2 cm in length. The actual material weights were recorded in each case so that the bulk volume and porosity could be calculated from the weighted average of the mineral grain densities. The approximate porosity of the synthetic sand was 35%.

The pressed synthetic sand samples were jacketed by wrapping the circumferential surface of the sample with Teflon tape. The samples were then placed in 3-mm-thick heat-shrink tubing and fitted with 2.5-cm-diameter end-caps. The tubing was shrunk around the sample, and the excess tubing trimmed. The jacketed samples were vacuum-saturated under brine (1000 ppm NaCl for this set of experiments) for about 1 h, followed by high pressure (134 bar, 2000 psi) brine saturation overnight.

Petrophysical Measurements

The saturated samples were then placed in a brine flow-saturation cell for permeability and electrical conductivity measurements (in part to monitor the saturation state of the sample) both before and after hydrothermal reaction. The samples were held with a confining pressure of 13.4 bar (200 psi), and a known flow rate of filtered (<5 μm), vacuum-degassed 1000-ppm NaCl brine was pumped through them. The pressure drop across the samples was measured using cal-

ibrated pressure transducers. The measurements were recorded by a dedicated computer which uses the data along with the sample dimensions, brine concentration and cell temperature to continuously calculate brine permeability and electrical conductivity. Measurements were made until constant values were attained, usually after several hours for unreacted samples and several days for reacted samples.
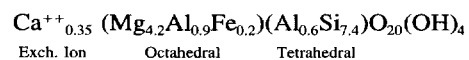
Analytical and Characterization Methods

The samples were characterized using a variety of methods. Mineralogy was determined using whole-rock and clay fraction XRD. Textural and morphological information was obtained using SEM, for both conventional air-dried (AD), and critical-point-dried (CPD) samples. SEM allows examination of specimens without the adverse effects caused by liquid surface tension (see McHardy and Birnie 1987, for a discussion of CPD sample preparation method).

Detailed chemical characterization of the smectite reaction product was determined by EMP analyses. These data were then used to calculate the composition and structural formula and to infer the CEC of the smectite, as well as the overall stoichiometry of the reaction. Dispersed specimens of the smectite were also examined by ED methods.

RESULTS

Reaction Mechanism

The mineralogy of the samples, as determined by whole-rock XRD (Figure 1), confirms the anticipated run products. The reactants (initial unreacted sample) consist of quartz, kaolinite and dolomite. The diffractogram of the products (reacted sample) shows that most of the dolomite has dissolved to form calcite and barely detectable smectite (whole-rock method). The smectite, along with some unreacted kaolinite, can be better observed in the clay fraction separate (<2 μm) XRD analysis (Figure 2). The precipitated smectite product consists mainly of silicon and Mg, with lesser amounts of Al and minor Fe (most likely from impurities within the dolomite and kaolinite), and Ca, as determined by EMP analyses (Table 2). This composition shows the importance of dolomite in the reaction, which is the source of Mg. The b unit cell dimension of the smectite is 9.203 Å, as determined from 060 ED measurements (Table 3, McHardy, personal communication), indicating that the smectite formed in the reaction is trioctahedral. The calculated whole unit cell structural formula of the smectite (saponite) is:

$$Ca^{++}_{0.35} \underbrace{(Mg_{4.2}Al_{0.9}Fe_{0.2})}_{\text{Octahedral}} \underbrace{(Al_{0.6}Si_{7.4})}_{\text{Tetrahedral}} O_{20}(OH)_4$$

Exch. Ion

The smectite formula can be used to estimate its CEC (Bain and Smith 1987), which was calculated to
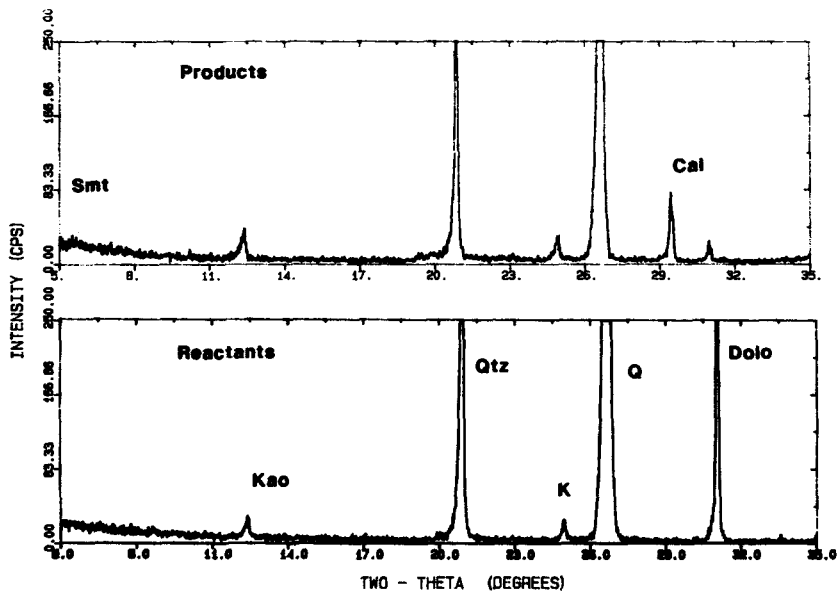
XRD Whole Rock

Figure 1.   Whole rock XRD: upper trace shows the products (reacted sample) of smectite and calcite relative to the reactants (initial sample, lower trace) of quartz (q), kaolinite (k) and dolomite.
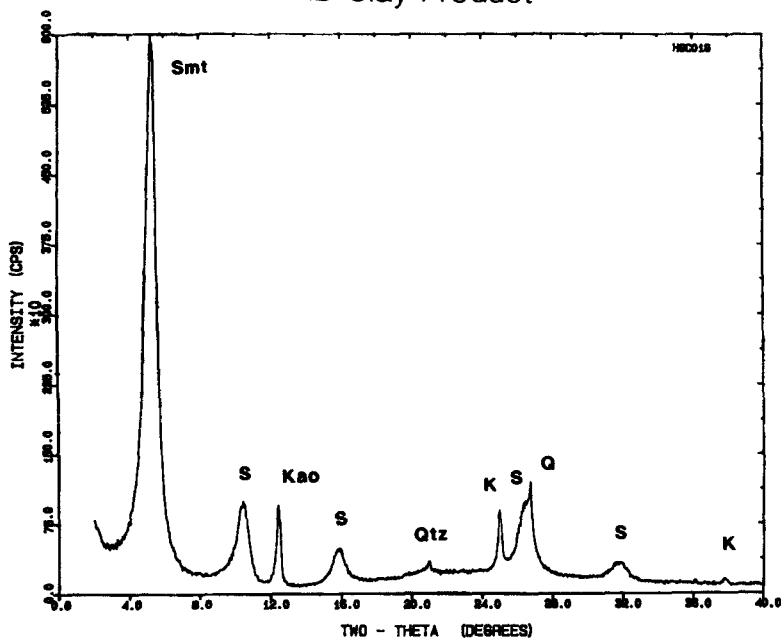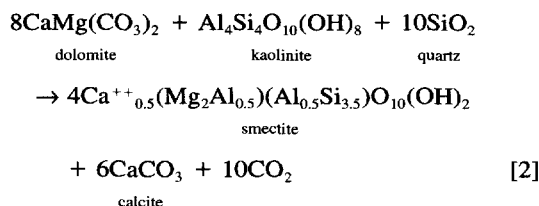
XRD Clay Product

Figure 2.   Clay fraction XRD (ethylene-glycol-solvated), of the run products showing maxima of smectite (Smt, S) as well as some kaolinite (Kao, K) and quartz (Qtz, Q).

Table 2. Smectite oxide composition based on EMP chemical analyses.

Oxide	Weight%	n	sd
SiO_2	53.4	11	0.9
Al_2O_3	9.3	11	0.4
MgO	20.6	11	1.6
Fe_2O_3	1.6	11	0.1
CaO	2.3	11	0.1
OH	13.0	—	—

Average analysis for smectite clay separate in wt%; n = number of analyses, sd = standard deviation.

Table 3. Smectite ED data: $d(060)$ polycrystalline ring spacing in Å, ref. = Al internal standard.

Negative	Dir. 1	Dir. 2	Dir. 3	b parameter
13625	1.531	1.530	1.531	9.184
13626	1.538	1.539	1.536	9.230
13627	1.533	1.532	1.533	9.196

Negative number = TEM Library, Macaulay Institute, Aberdeen, Scotland (W. J. McHardy, personal communication).

be 100 meq/100 g (a common value for smectite and a much larger value than any of the reactants), as well as the stoichiometry of the reaction. The generalized result gives:

$$8CaMg(CO_3)_2 + Al_4Si_4O_{10}(OH)_8 + 10SiO_2$$
$$\text{dolomite} \qquad\qquad \text{kaolinite} \qquad\qquad \text{quartz}$$

$$\rightarrow 4Ca^{++}{}_{0.5}(Mg_2Al_{0.5})(Al_{0.5}Si_{3.5})O_{10}(OH)_2$$
$$\text{smectite}$$

$$+ 6CaCO_3 + 10CO_2 \qquad\qquad [2]$$
$$\text{calcite}$$

Note that for simplification, a generalized half unit cell smectite formula has been used for the above calculation.

The reaction is dominated by dolomite dissolution, which provides Mg for smectite and Ca and CO_3 for calcite, as well as generating significant amounts of CO_2 (the exchangeable cation for smectite is assumed to be Ca^{++}, also from dolomite). Kaolinite provides all of the Al and some of the Si for smectite, and the remainder of the Si is provided by quartz (about 70%). This final point is supported by the fact that no Al oxide/hydroxide phases have been observed in the run products, which would be expected if kaolinite provided all the Si for the reaction. Therefore, quartz provides substantial amounts of Si for smectite growth. The above reaction shows that a synthetic sandstone with 5% dolomite and 5% kaolinite can form not more than approximately 5 wt% smectite. CEC measurements on the run products indicate that the actual maximum contents formed are in the 2 to 3 wt% range.

Diagenetic Clay Morphology

SEM observations of CPD-reacted samples show that the smectite occurs as a delicate and pervasive microporous cement, with a complex pore-bridging texture affecting most of the available pore space. A graphic display of these changes in the sandstone is shown in Figure 3, relative to a control sample of 100% quartz in which no clay has formed (Figure 3a). Figure 3b shows the morphology of clay formed during the early stages of the reaction. Note the extremely small and thin individual clay particles growing out

into the pore space. Figures 3c and 3d show extensive clay formation, often bridging the entire pore space.

Morphologically, the clay is similar to naturally occurring diagenetic smectite from a Texas Gulf Coast Oligocene Frio sandstone reservoir (Figures 4a and 4b), which also shows a pervasive pore-bridging distribution. The delicate synthetic clay texture collapses during air-drying and forms irregular pore-lining "anastomosing" aggregates (Figures 3e and 3f). This phenomenon is similar to that observed for the air-dried Frio reservoir samples (Figures 4c and 4d).

Permeability

After reaction, brine permeability reductions of up to 98% were observed from the growth of not more than approximately 5 wt% smectite (Figure 5). This dramatic reduction is related to the complex pore-bridging texture of the clay which affects much of the available pore space. An air-dried sample (dried at 110 °C for 2 d), followed by brine resaturation, showed a marked increase in permeability. This increase is associated with the collapse of the clay texture noted above (Figures 3e and 3f) and confirms the relationship between clay morphology and sandstone permeability, even at very low clay contents. The synthetic sandstones studied here are primarily composed of very fine sand size quartz grains, and the reader should use caution in directly applying these results to coarser-grained lithologies.

DISCUSSION

The experimental results provide valuable insights into the effects of diagenetic clay minerals on rock properties. It is important for the sake of this discussion to bear in mind the distinction between diagenetic clay minerals and siliciclastic shale components, which also alter rock properties and often constitute the main source of detrital clay minerals in reservoir sands. The experiments provide a controlled method of isolating the effect of diagenetic clays, such as illite, mixed-layered clays and smectite, on rock properties.

Reservoir Quality

The most significant finding of this study is the large permeability reduction effect that such pervasive diagenetic clay can have on reservoir sands. This confirms observations reported by production operations
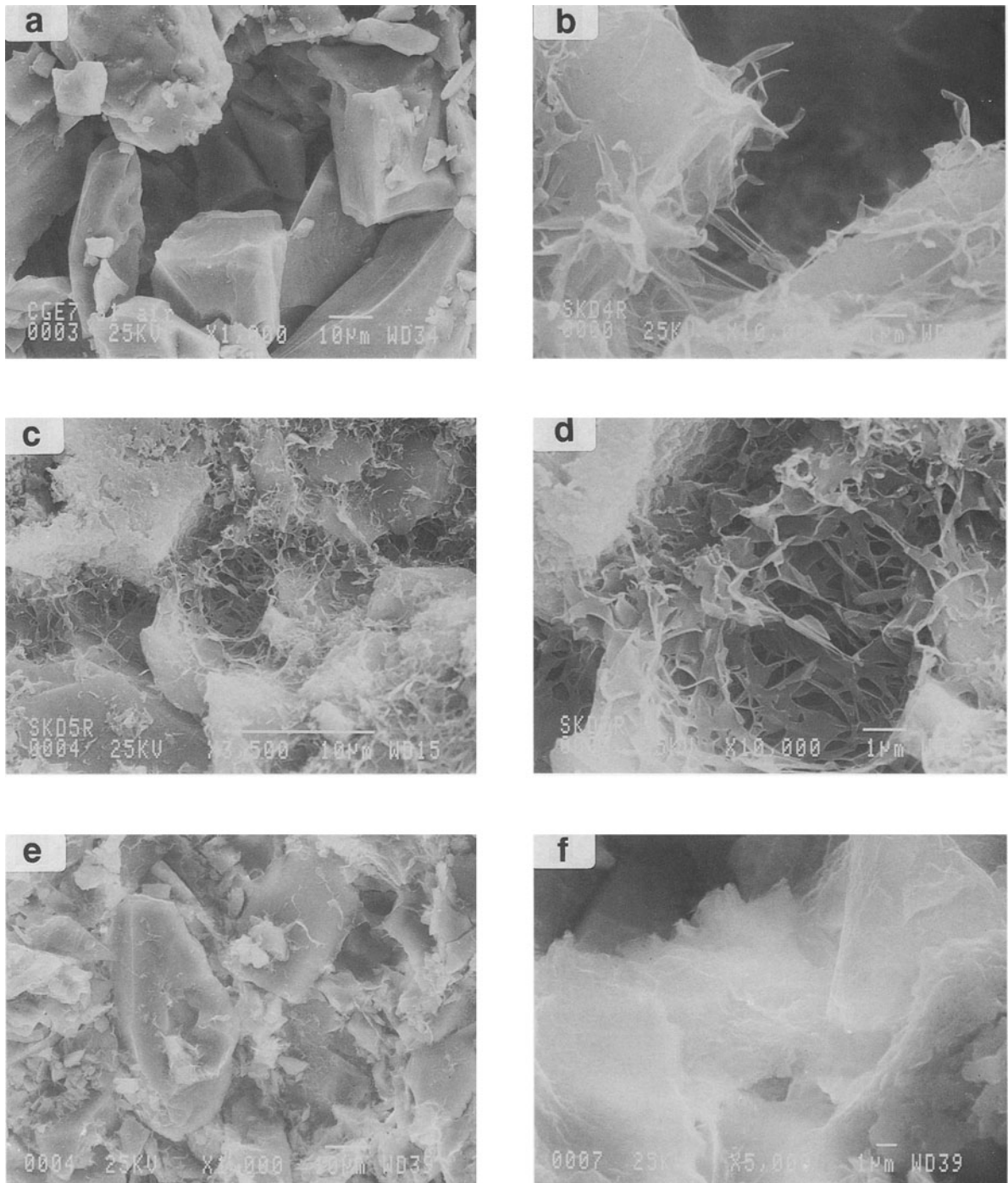
Figure 3.   SEMs of a control (Figure 3a, 100% quartz) and reacted samples. Figure 3b shows incipiently formed smectite clay. The small individual clay particles are extremely thin, showing the clay at its earliest stages of growth. Note the delicate, microporous, pore-bridging smectite morphology occluding most of the available pore space in Figures 3c and 3d. Figures 3e and 3f show the collapsed clay in an air-dried sample. Note the thin pore-lining irregular masses of the collapsed smectite.

in fields with these types of clays present (Heaviside et al. 1983; Pallatt et al. 1984; Bushell 1986; and deWaal et al. 1988). The previous examples primarily relate to the effects of illitic clays. The results here demonstrate that similar effects can also be expected for reservoirs with diagenetic smectite as well as other mixed-layered clays. The results also show that smectites, like illite and mixed-layered illite–smectite, are
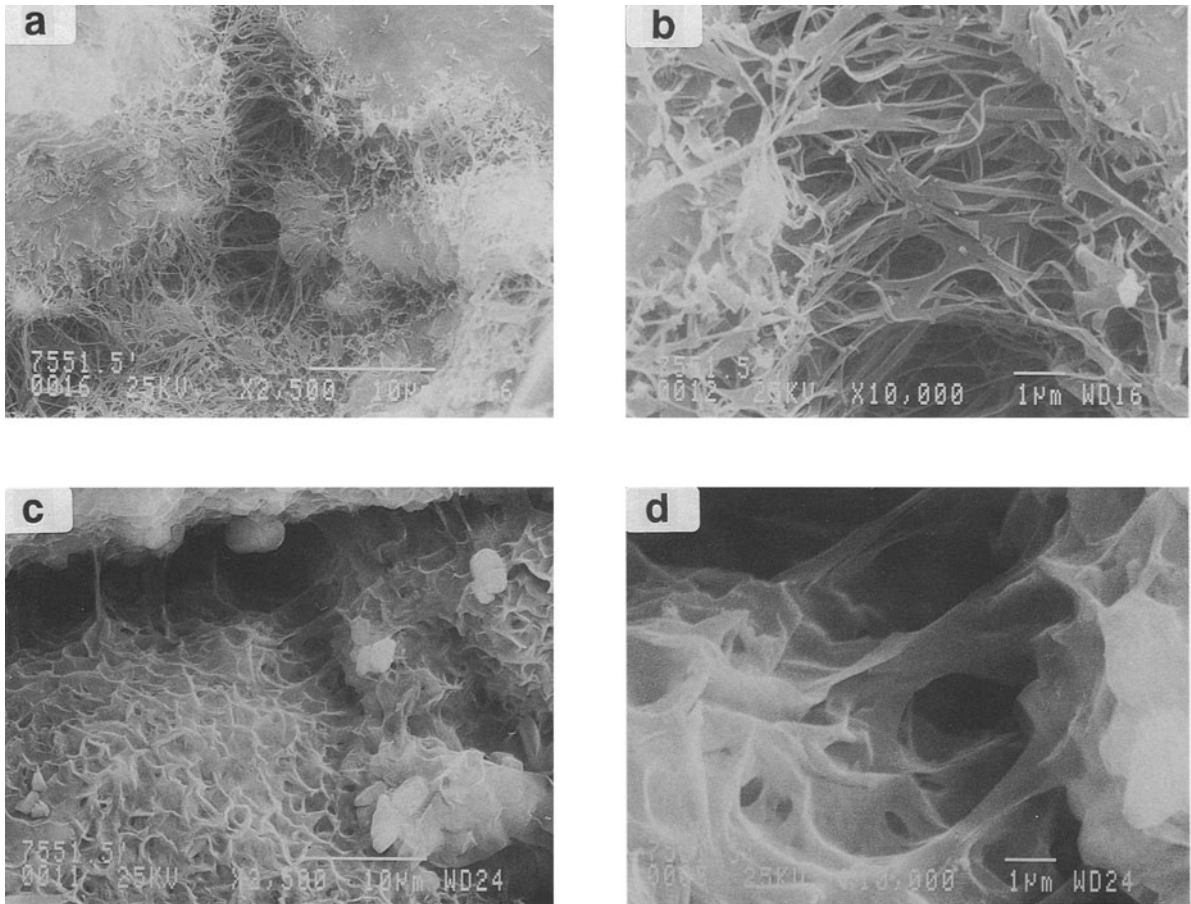
Figure 4.   SEMs of preserved reservoir smectite cements (Oligocene Frio sandstone, Texas Gulf Coast). Critical-point-dried (CPD) sample preparations (a, b) versus conventional air-dried (AD) samples (c, d). Note the similarity of the delicate clay morphology of the synthetic sample (c, d). Note also the collapse of the clay into irregular pore-lining masses with conventional air-drying methods (for implications, see text).

susceptible to collapse on air-drying. One consequence of this behavior is that conventional core petrophysical measurements may not fully reflect the effects of these clays on rock properties. It is also important to note
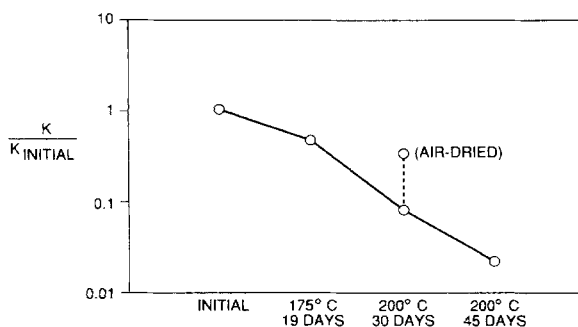

Figure 5.   Relationship between brine permeability and synthetic clay reaction conditions. Note the log permeability scale and the large reductions in normalized brine permeability relative to the initial value.

that this collapse morphology (Figure 4d) is similar to that commonly thought typical of "pore-lining" authigenic smectite (compare Wilson and Pittman 1977, their Figure 17). Although this morphology is useful for descriptive purposes, workers should be aware that it may not accurately represent the true habit of the clay in subsurface reservoirs.

The results can also be used to estimate the amount of microporous formation brine or "ineffective porosity" associated with the clay (Nadeau and Hurst 1991; Hurst and Nadeau 1995). Here, the value can be obtained by assuming that the permeability reduction is related to a decrease in effective porosity (using a generalized clean sand trend after Beard and Weyl 1973). In this case the data indicate a value of 15 porosity units (Figure 6) based on the largest experimentally observed permeability reduction (Figure 5). By assuming that this reduction is caused by the growth of 5% clay, the equation for estimating the clay microporosity can be used, and is given by:
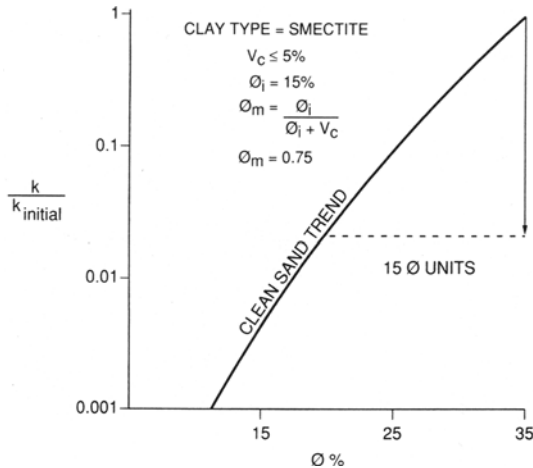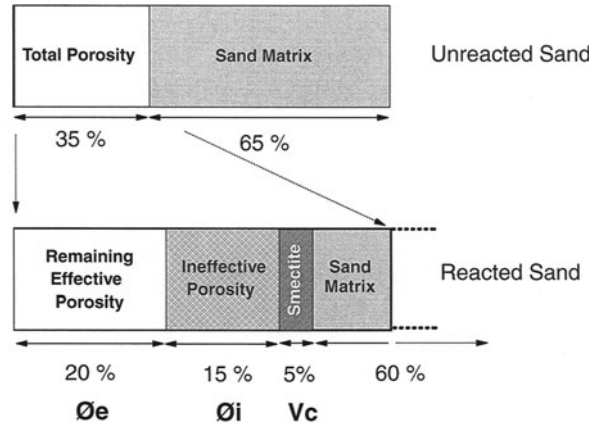
Figure 6.   Illustration showing the estimation of clay microporosity, ϕ_m, from the maximum experimentally observed permeability reduction (Figure 5). The ineffective porosity, ϕ_i, is related to a reduction in effective porosity relative to a generalized porosity/permeability clean sand trend (after Beard and Weyl 1973). The extrapolated value of ϕ_i is 15%. The amount of clay, V_c, is taken as 5% (see text). This estimate gives a value for ϕ_m of 0.75, or 75%.

Øe = Effective porosity
Øi = Ineffective porosity estimated from
        permeability reduction (Fig. 6)
Vc = Volume of diagenetic clay formed from the
        dissolution of sand matrix components.

Figure 7.   Illustration showing a simplified "box model" of sand matrix, porosity, diagenetic clay formation and clay microporosity from the estimate value of 0.75 or 75% (Figure 6). Note that the diagenetic clay forms from the dissolution of sand matrix components, and is thus analogous to "closed" system diagenesis.

$$\phi_m = \phi_i/(\phi_i + V_c) \qquad [3]$$

where ϕ_m is the clay microporosity, ϕ_i is the ineffective volume or clay bound water, and V_c is the mineral or solid volume of the clay. The estimate of ϕ_m gives a microporosity value of 0.75, or 75%. This means that for every mineral volume of clay grown, at least 3 pore volumes of the sand have been rendered ineffective. It should be recalled that the maximum amount of smectite that could be formed in the experiments was 5 wt%, and that the mineral volume percent in a sandstone with 35% porosity will be significantly less. Therefore, the 75% value, acknowledging the uncertainties associated with its derivation, is arguably a minimum figure and consistent with the SEM observations of the clay showing it to form a delicate and highly microporous cement (Figures 3c and 3d). If, for example, the actual solid mineral volume of smectite formed was 2%, then the microporosity estimate would be 88%. It is also important to note that the 75% value is much larger than would have been inferred from a simple consideration of smectite interlayer water (20 to 35%, depending on the interlayer cation) which is more appropriate for the collapsed state, or if the smectite was assumed to be present within relatively compacted detrital shale components. Preferable to the method above, capillary pressure measurements of the clay bound water in reacted samples would provide a more detailed characterization of the diagenetic smectite effect on rock properties.

Another important aspect of the experimental system is that although the synthetic diagenetic clay formed within the sand porosity, the reactant components were not "imported" into the sand. The diagenetic clay formed from the dissolution of mineral component reactants within the sand matrix. This can be illustrated by a simplified "box model" of the synthetic sands along with the interpreted results (Figure 7), and represents the geochemical conditions within a "closed" system. In this regard the reaction is similar to that proposed for the isochemical formation of diagenetic illite in sandstone reservoirs from the dissolution of kaolinite and K-feldspar reactants (Bjørlykke 1983; Bjørkum and Gjelsvik 1988; Ehrenberg and Nadeau 1989).

Experimental Petrophysics

The experimental techniques outlined here can be applied to several areas of interest to geoscientists and the petroleum industry. Understanding the effect of clay minerals on the electrical properties of reservoirs is important in evaluating their hydrocarbon content and productivity from well logging measurements (Ellis 1987). Commonly used models attempt to correct for the excess conductivity attributable to clay components as a function of CEC (Waxman and Smits 1968), but a definitive basis for calculating hydrocarbon saturation from electrical measurements has not yet been developed. The experimental methods shown here can allow detailed measurements of rock properties under controlled

conditions and known changes in clay content. Therefore, these methods can be applied to produce more accurate petrophysical models of diagenetic clay mineral effects.

The relatively low temperature and short reaction times for the growth of smectite from the common sedimentary minerals—dolomite, kaolinite and quartz—make this reaction a likely occurrence during steam flood operation. The reaction mechanism observed here is virtually identical to those found by experimental core steam flood experiments using Alberta heavy-oil sand Clearwater Formation materials (Kirk et al. 1987). They also showed marked permeability reductions that were applicable to steam flood enhanced oil recovery operations. The experimental approach outlined here may also provide technical support for well stimulation methods in reservoirs and other lithologies prone to formation damage by induced clay mineral reactions.

The occurrence of overpressure or geopressure at certain depths in sedimentary basins has been correlated with the formation of diagenetic clay (illite) in shales (Burst 1969). The mechanism by which this occurs is uncertain, however, and could be related to a number of factors. The experimental results shown here suggest that dispersed diagenetic clays such as smectite and illite alter rock properties by forming pervasive microporous cements, which are capable of greatly reducing formation permeability. Although the results shown here are for reservoir sandstones, they provide some insights regarding the effects of clay diagenesis in finer-grained lithologies, which would seemingly be even more susceptible to this mechanism of permeability reduction given their smaller pore sizes. Therefore, the effects reported here may also provide important petrophysical models of clay diagenesis for evaluating subsurface rock properties used in sedimentary basin analysis of fluid pressure and migration (Harrison and Summa 1991; Hermanrud 1993; Bjørkum and Nadeau 1996).

Other parameters of experimental petrophysical interest include variations in reactant and formation water chemistry, which are considered to be influential in clay mineral diagenesis (Hurst and Irwin 1982). Preliminary results have already shown that the addition of siderite ($FeCO_3$) to the reaction mix results in the formation of pore-lining chlorite-like Fe-bearing clay cements (compare Hutcheon 1984). Such clays have been attributed to anomalously good reservoir quality in deeply buried reservoirs (Ehrenberg 1993). Therefore, a wide variety of clay minerals and reaction conditions can be readily studied by these methods which are relevant to a number of topics of scientific and industrial interest.

CONCLUSIONS

The experimental results of this study have shown that:

1) Large reductions in sand permeability are associated with the growth of not more than 5 wt% smectite clay.
2) The mechanism for permeability reduction is related to the morphology of the microporous clay cement.
3) The clay morphology collapses on air-drying.
4) Commonly observed pore-lining smectite morphology in reservoir sandstones may be an artifact of conventional sample preparation methods.
5) Conventional core analysis measurements of samples containing diagenetic smectite may not be representative of subsurface reservoir properties.
6) Experimental petrophysics is a useful research method for determining the effects of diagenetic clay on rock properties.

REFERENCES

Bain DC, Smith BS. 1987. Chemical analysis. In: Wilson MJ, editor. A handbook of determinative methods in clay mineralogy. London: Blackie. p 248–274.

Beard DC, Weyl PK. 1973. Influence of texture on porosity and permeability of unconsolidated sand. Am Assoc Petrol Geol Bull 57:349–369.

Bjørkum PA, Gjelsvik N. 1988. An isochemical model for the formation of authigenic kaolinite, K-feldspar, and illite in sediments. J Sed Petrol 58:506–511.

Bjørkum PA, Nadeau PH. 1996. A kinetically controlled fluid pressure and migration model. Am Assoc Petrol Geol Ann Conv Proc Abstr. p A15.

Bjørlykke K. 1983. Diagenetic reactions in sandstones. In: Parker A, Sellwood W, editors. Sediment diagenesis. Dordrecht: Reidel. p 169–213.

Burst JF. 1969. Diagenesis of Gulf Coast clayey sediments and its possible relation to petroleum migration. Am Assoc Petrol Geol Bull 53:73–93.

Bushell TP. 1986. Reservoir geology of the Morecambe Field. In: Brooks J, Goff J, van Hoorne B, editors. Habitat of Paleozoic gas in N. W. Europe. Geol Soc Spec Publ 23. p 189–208.

deWaal JA, Bil KJ, Kantorowicz JD, Dicker AIM. 1988. Petrophysical core analysis of sandstones containing delicate illite. The Log Analyst 29:317–331.

Ehrenberg SN. 1993. Preservation of anomalously high porosity in deeply buried sandstones by grain-coating chlorite: Examples from the Norwegian Continental Shelf. Am Assoc Petrol Geol Bull 77:1260–1286.

Ehrenberg SN, Nadeau PH. 1989. Formation of diagenetic illite in sandstones of the Garn Formation, Haltenbabken area, Mid-Norwegian Continental Shelf. Clay Miner 24: 233–253.

Ellis DV. 1987. Well logging for earth scientists. New York: Elsevier. 532 p.

Harrison WJ, Summa LL. 1991. Paleohydrology of the Gulf of Mexico Basin. Am J Sci 291:109–176.

Heaviside J, Langley GO, Pallatt N. 1983. Permeability characteristics of Magnus reservoir rock: Paper A. London; 8th European Formation Evaluation Symp. p 1–29.

Hermanrud C. 1993. Basin modelling techniques—An overview. In: Doré AG, Auguston JH, Hermanrudd C, Stewart DJ, Sylta Ø, editors. Basin modelling advances and applications. Norwegian Petroleum Soc Spec Publ 3. Amsterdam: Elsevier. p 1–34.

Hurst A, Irwin H. 1982. Geological modeling of clay diagenesis in sandstones. Clay Miner 17:5–22.

Hurst A, Nadeau PH. 1995. Clay microporosity in reservoir sandstones: An application of quantitative electron microscopy in petrophysical evaluation. Am Assoc Petrol Geol Bull 79:563–573.

Hutcheon I, 1984. A review of artificial diagenesis during thermally enhanced recovery. In: McDonald DA, Surdam RC, editors. Clastic diagenesis. Am Assoc Petrol Geol. Memoir 37. Tulsa. p 413–429.

Kirk JS, Bird GW, Longstaffe FG. 1987. Laboratory study of the effects of steam-condensate flooding in the Clearwater Formation: High temperature flow experiments. Can Soc Petrol Geol 35:34–47.

McHardy WJ, Birnie AC. 1987. Scanning electron microscopy. In: Wilson MJ, editor. A handbook of determinative methods in clay mineralogy. London: Blackie. p 174–208.

McHardy WJ, Wilson MJ, Tait JM. 1982. Electron microscope and X-ray diffraction studies of filamentous illitic clay from sandstones of the Magnus Field. Clay Miner 7: 23–29.

Nadeau PH, Hurst A. 1991. Application of back-scattered electron microscopy to the quantification of clay mineral microporosity in sandstones. J Sed Petrol 61:921–925.

Pallatt N, Wilson MJ, McHardy WJ. 1984. The relationship between permeability and the morphology of diagenetic illite in reservoir rocks. J Petrol Technol 36:2225–2227.

Waxman MH, Smits LJM. 1968. Electrical conductivities in oil-bearing shaly sands. Soc Petrol Eng J 243:107–122.

Wilson MD, Pittman ED. 1977. Authigenic clays in sandstones: Recognition and influence on reservoir properties and paleo-environmental analysis. J Sed Petrol 47:3–31.